EXPERIMENTAL STUDY ON ICE ACCUMULATION BEFORE INVERTED SIPHON

HUI FU[1], XINLEI GUO[1], PENG WU[2], TAO WANG[1], YONGXIN GUO[1], JIAZHEN LI[1]

[1] State Key Laboratory of Simulation and Regulation of Water Cycle in River Basin, China Institute of Water Resources and Hydropower Research, Beijing, China
fuhui_iwhr@126.com; guoxinlei@163.com; taozy163@163.com
[2] Environmental Systems Engineering, University of Regina, Regina, Canada
peng.wu@uregina.ca

ABSTRACT

In the vast northern regions, ice accumulation or ice cover may form along rivers in winter, which may cause ice jam flood. For water diversion project, ice related problems may increase flow resistance or even cut off water supply which has considerable influences. This paper takes the Tanghe inverted siphon of the Middle Route of the South-to-North Water Diversion Project in China as an example, and carries out experimental studies under the real ice condition with different water levels, flow discharges and submerged depths. The characteristics of the ice jam distribution and the relationship between t_i/H(ratio of ice jam thickness t_i to total water level H) and Fr_i(Froude number under ice jam) are analyzed. An equation for the ice jam thickness calculation before the inverted siphon is also put forward.

Keywords: Inverted siphon, Ice jam, Ice thickness, Water diversion project

1   INTRODUCTION

For open channel water diversion projects in northern China, the ice jam is an important issue in winter. Examples of such projects include the Water Diversion Project from Yellow River to Qingdao City, the Water Diversion Project from Yellow River to Tianjin City and the Middle Route of the South-to-North Water Diversion Project(Fu et al., 2010). The Middle Route of the South-to-North Water Diversion Project is one of the biggest water diversion projects in China and water flows from warmer area to cold area, the length of which is about 1277 kilometers. The red line in Figure 1 shows the channel route of the project (Zhang et al., 2014). And Figure 2 shows ice problems in the channel (Credit: Yang, J.B.). Inverted siphons are commonly used in water diversion projects. Once one of them is jammed along the channel, the safe operation of the whole project will be threatened. Inverted siphons usually were reported to be jammed by ice, such as the inverted siphons of the Shahe irrigation district in 2003 and the water diversion project from Yellow River to Baiyangdian in 2008. For preventing inverted siphons from ice jam, the discharge of the Beijing-Shijiazhuang section in the Middle Route of the South-to-North Water Diversion Project was reduced to about 10 m^3/s, only 1/6 of the design discharge. So the water diversion efficiency of the water diversion projects is significantly lowered during the ice period.

Figure 1. Location of the middle route of the Middle Route of the South-to-North Water Diversion Project.

At present, the safe operation of inverted siphons during ice period is not well studied, apart from the studies of ice transportation through a submerged gate(Fu et al., 2013a; Ashton, 2008). The ice jam formation and the thickness distribution are issues to be explored for inverted siphons. To prevent the ice jam, a conservative value of Froude number was usually used for the safe operation of inverted siphons(Beltaos et al., 2012; Shen, 2010; Guo et al, 2013; Dow et al, 2011; Ashton, 2011), which would sharply decrease the water transfer capacity in winter. So a better understanding of the ice jam thickness along the channel is urgently desirable.

With Tanghe inverted siphon of the Middle Route of the South-to-North Water Diversion Project in China as an example, the ice accumulation processes before the inverted siphon were tested under the real ice condition by the experiment platform of China Institute of Water Resources and Hydropower Research(Fu et al., 2013b). The characteristics of the ice jam distribution and the relationship between t_i/H and Fr_i were analyzed in this paper. And then an equation for the ice jam thickness calculation before an inverted siphon was put forwarded.

<div align="center">

(a) Ice floes   (b) Ice jam

Figure 2. Ice problems of the Middle Route of South-to-North Water Diversion Project
</div>

2   EXPERIMENTAL SET UP AND CASES

A series of experiments are conducted in a flume of 50 m long, 0.8 m wide and 0.8 m high. A 6 m long inverted siphon is used to model the typical Tanghe inverted siphon, and the model scale is 1:23.4 (according to the width of the flume and the prototype dimension of Tanghe inverted siphon). Because of the limitation of the laboratory length, the horizontal length of the inverted siphon model is shortened. And the height of the inverted siphon inlet is 0.244 m. Ice pieces of average dimension of 0.276 m×0.0186 m× 0.0025 m are used to model the ice accumulation and the transportation at the inlet of the inverted siphon. The use of a real ice material can overcome many disadvantages of plastic and paraffin, such as the friction coefficient, the adhesiveness, and the soakage (Matsumoto et al, 2014; Wang et al, 2011, 2015). The detailed arrangement of the inverted siphon and the flume is shown in Figure 3, where H_1 is the submerged depth from the water surface to the top of the inlet. A thickness measuring section is set every 0.1 m, with nineteen sections before the inlet of the inverted siphon.

The real ice experiment platform is automatically operated, and it consists of the control computer, the DDC device drive and the data collecting module, the axial flow fans, the centrifugal fans, the heating system, the temperature feed-back system, 9 refrigeration units and so on. 27 high-accuracy temperature sensors are distributed along the platform to provide real-time temperatures for the temperature control system. By an air temperature control system, the lowest laboratory temperature can be reduced to −15ºC, with a control accuracy of ±0.5ºC and the temperature fluctuation of less than 1ºC.

(a) Experimental flume
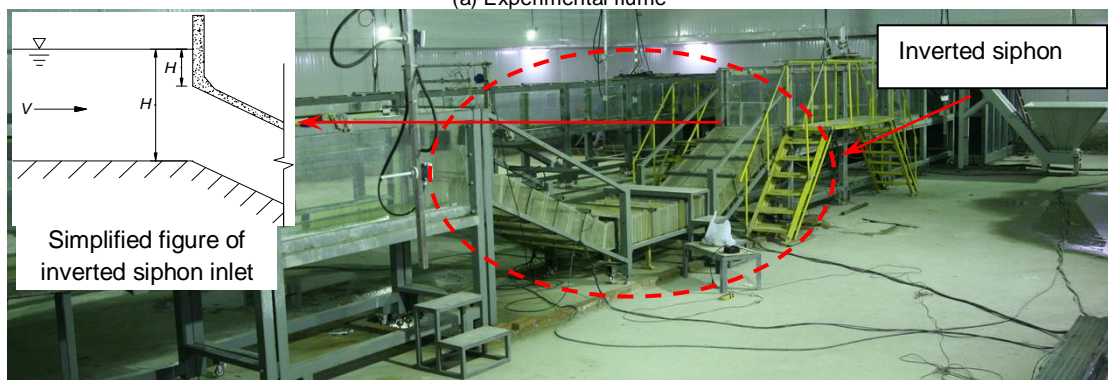
(b) Inverted siphon

Figure 3. Layout of experimental flume and inverted siphon experiment

49 ice accumulation cases are tested. The value of *H* is in the range between 0.254 m and 0.354 m, the flow discharge *Q* is in the range between 13.1 L/s and 54.4 L/s. And the incoming ice discharge is 0.12 L/s, which is enough for the ice jam accumulation. All experiment cases are shown in Table 1. These cases cover the normal operation conditions of inverted siphons in the Middle Route of the South-to-North Water Diversion Project.

Table 1. Experiment cases

| No	Water depth(m)	Discharge(m³/s)	Mean flow velocity(m/s)	No	Water depth(m)	Discharge(m³/s)	Mean flow velocity(m/s)
1	0.254	19.6×10^{-3}	0.097	10	0.314	29.3×10^{-3}	0.117
2	0.264	13.1×10^{-3}	0.062	11	0.314	36.4×10^{-3}	0.146
3	0.264	21.3×10^{-3}	0.101	12	0.324	41.1×10^{-3}	0.160
4	0.279	26.1×10^{-3}	0.118	13	0.334	39.5×10^{-3}	0.149
5	0.284	23.0×10^{-3}	0.102	14	0.344	46.2×10^{-3}	0.169
6	0.289	28.3×10^{-3}	0.123	15	0.354	42.6×10^{-3}	0.151
7	0.294	28.3×10^{-3}	0.121	16	0.354	46.6×10^{-3}	0.166
8	0.304	31.0×10^{-3}	0.128	17	0.354	49.7×10^{-3}	0.177
9	0.309	34.4×10^{-3}	0.140				

3   ICE ACCUMULATION CHARACTERISTICS

In the actual project, the water surface is higher than the top of the inverted siphon inlet, so the submerged ice will not enter the inverted siphon immediately and continue to accumulate at the inlet unless the water transportation capacity is high enough. The shape of the inverted siphon inlet also influences the vertical velocity distribution. The upper flow velocity before the inverted siphon is smaller and the location of the maximum velocity is closer to the channel bed(Figure 4), which is much different from the common open water flow or the ice covered flow(Sui et al., 2010; Beltaos, 2008; Yamazak et al, 2014). Under the influences of

above factors, the ice accumulation and its distribution before the inverted siphon have their own characteristics.
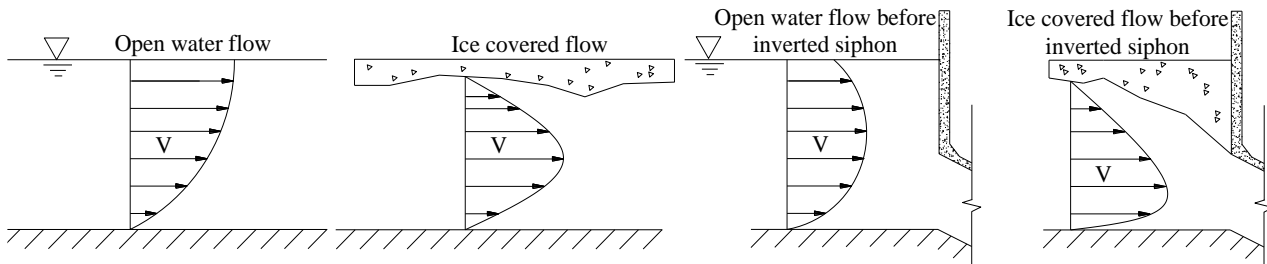

Figure 4. Vertical velocity distribution

Under the same flow discharge condition, the smaller the water depth, the larger the ice jam thickness becomes. This is because a smaller water depth means a higher Froude number when the flow discharge is fixed, and a larger ice jam thickness is needed to balance the water thrust (Figure 5). Similarly, under the same water level condition, a larger flow discharge leads to a larger ice jam thickness(Figure 6). But the largest ice jam thickness is not found at the critical case that the ice is just not transported into the inverted siphon. When the ice transportation discharge of the channel is less than the upstream incoming ice discharge, the ice jam will be thickened. After the flow discharge is increased to a certain level, along with the enhanced water thrust, more ice will be transported downstream, and the ice jam thickness tends to de crease, the leading edge of the ice jam will also not be developed upstream. Figure 7 shows the ice jam thickness distribution under different flow discharge conditions when the water depth H=0.345m. It is obvious that the ice jam thickness when Q=46.6L/s is larger than that when Q=42.6L/s, but when Q increases to 49.7 L/s, the ice jam thickness decreases (where S is the distance from the inlet of the inverted siphon). Overall, the maximum ice jam thickness is close to the submerged depth (H_1). This is because when the ice jam thickness is greater than the submerged depth (H_1), the adhesiveness among the ice is hard to balance the drag force of the water.
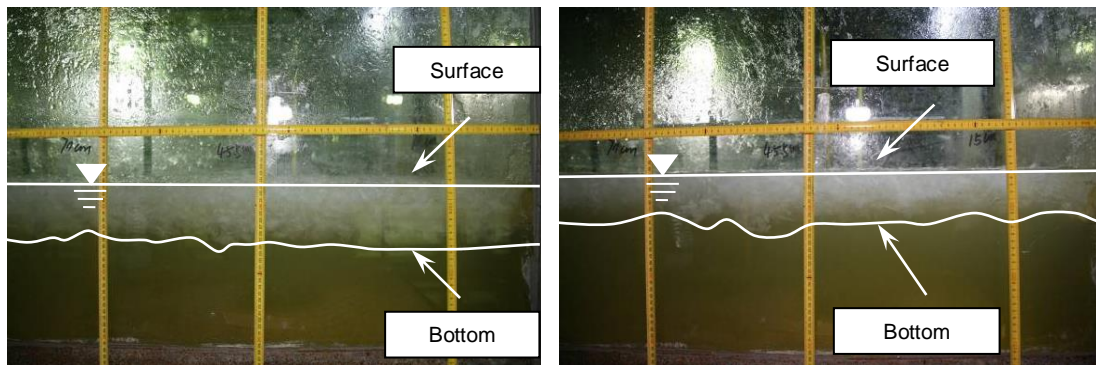
(a) H=314mm, Q=41.7L/s

(b) H=334mm, Q=41.7L/s
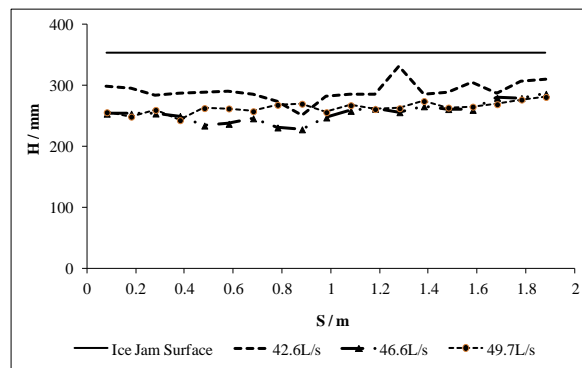
Figure 5. Ice jam distribution before inverted siphon (constant value of Q with different H)
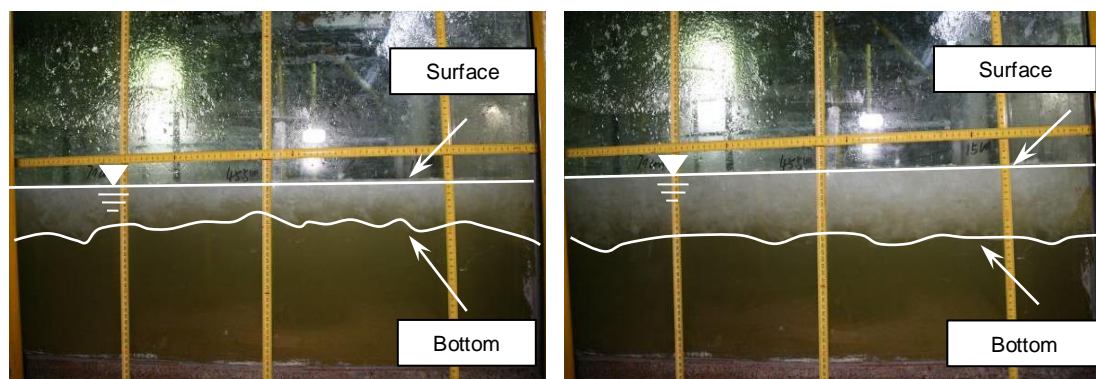
(a) H=354mm, Q=42.6L/s

(b) H=354mm, Q=49.7L/s

Figure 6. Ice jam distribution before inverted siphon (constant value of H with different Q)
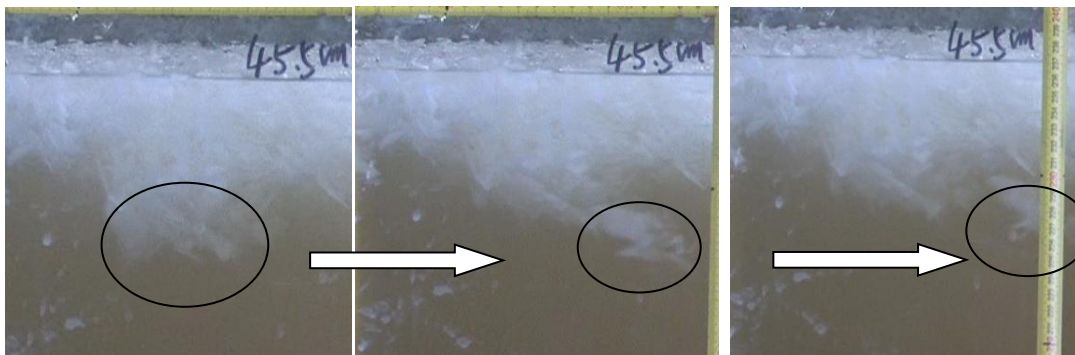
Figure 7. Ice jam thickness distribution under different flow discharge conditions (H=0.345m)

From the real ice experiments, it is found that the ice accumulates as "ice ball" and then transports under ice jam. Along with the increase of the Fr value, the viscosity between ice cannot resist drag force of water, the big "ice ball" can break up into small "ice ball", and then a part of "ice ball" stay in situ and other transports under ice jam(Figure 8). The above phenomenon influences the critical condition of ice transportation.

(a) Under low Fr value condition, ice transports as "ice ball"（H=279mm, Q=25.2L/s, Fr=0.069）

(b) Under high Fr value condition, big "ice ball" breaks up into small "ice ball"
（H=354mm, Q=49.7L/s, Fr=0.095）
Figure 8. Transportation of "ice ball" under different Fr value conditions

For the distribution of the ice jam thickness along the channel, the upstream thickness is slightly less than that downstream. One reason may be that the ice jam turns the open water flow to an ice covered flow and the area of the flow section is also reduced, so the water depth along the channel increases and then the Froude number of the channel will decrease along with the development of the ice jam. In critical cases, when the water depth H=0.254 m-0.304 m, 0.309 m-0.334 m and 0.339 m-0.354 m, the average ice jam thickness along channel is about 0.02 m-0.04 m, 0.04 m-0.06 m and 0.05 m~0.10 m, respectively.

Along with the increasing value of (H_1/H), the critical Froude number increases, which is used to judge if the ice is transported or not. At a low submerged depth (H_1), the critical Froude number is about 0.06, at a high submerged depth (H_1), the critical Froude number can be increased to 0.08-0.09. Obviously, the large submerged depth H_1 is not advantageous for the ice transportation downstream. Along with the increase of the submerged depth (H_1), a greater force is needed to overcome the buoyancy and the increased transportation distance.

4   ICE THICKNESS CALCULATION ALONG CHANNEL

The larger the Froude number under the ice jam Fr_i, the larger the ice jam thickness is needed to balance the water thrust. So the ice jam thickness is closely related to the Froude number under the ice jam. In our experiments, the value of (H_1/H) varies from 0.039 to 0.330, and Fr (Froude number of open channel upstream) ranges from 0.039 to 0.109. It is obvious that the ice jam thickness before the inverted siphon is closely related to the total water depth H (when H is fixed, it is related to the submerged depth H_1= H-0.244) and the Froude number under the ice jam Fr_i. According to the plots of t_i/H versus Fr_i of all experiment cases, the following linear equation is found to describe the relationship between t_i/H and Fr_i (Fu et al., 2017).

$$\frac{t_i}{H} = k(Fr_i) + b \qquad\qquad [1]$$

where k and b are coefficients, varying with the distance from the inlet of the inverted siphon.

The mean values of t_i/H and Fr_i in all cases are shown in Figure 9. It shows that with the increase of Fr_i, the critical t_i/H is also increased. For the section which is closer to the inlet of the inverted siphon, the values of k and b are larger, on the other hand, the values are smaller for the section away from the inlet of the inverted siphon. This is because the ice jam thickness at the section near the inlet is larger than that at the section far away from it. Symbol × represents the critical case in Figure 9. In a low submerged depth case, the value of the critical Fr_i is about 0.07-0.08, in a high submerged depth case, the value of the critical Fr_i is about 0.10-0.12. Figure 9 shows that Eq. [1] can fit the measured data well, which can be used to predict the ice jam thickness along the channel by coefficients shown in Table 1.
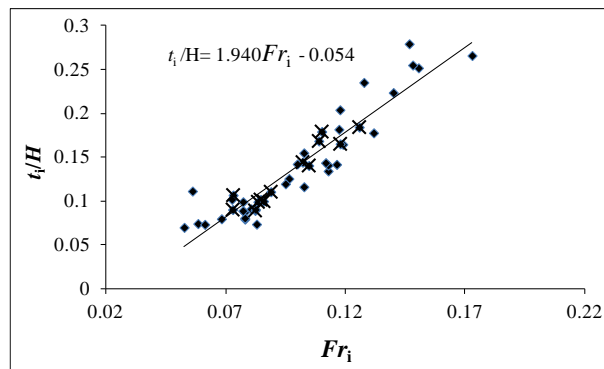

Figure 9. The comparison of measured data and calculations

It is interesting that our experiment results have a similar tendency as those at the upper Hequ reach of the Yellow River (1982-1989) and St. Lawrence River (1947-1950)(Sui et al, 2002,2005; Michel, 1984). For St. Lawrence River, the Froude number under the ice jam is between 0.05 and 0.25, which is also similar to our experiments (Figure 10). For the upper Hequ reach jam, the larger the value of Fr_i, the larger the value of t_i/H will be, but for the lower Hequ reach jams, as Fr_i increases, t_i/H decreases (Figure 11). One main reason may be that after the formation of the upper ice jam, the ice supply for the lower reach is decreased. Along with a larger Froude number, the water transport capacity is larger and may exceed z the incoming ice supply, so Fr_i increases, t_i/H decreases for the lower Hequ reach. This shows that the ice discharge also plays an important role in the ice jam process.
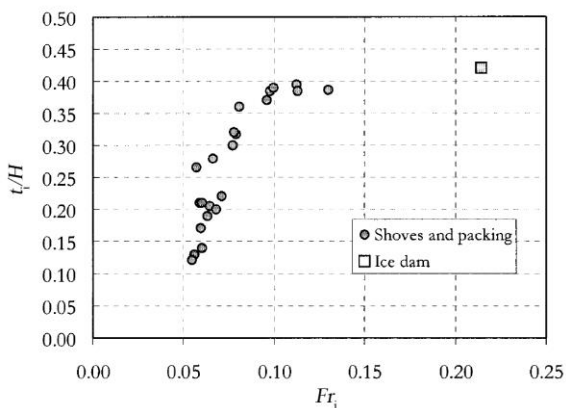
Figure 10. Relationship between
Fr_i and t_i/H of St. Lawrence River
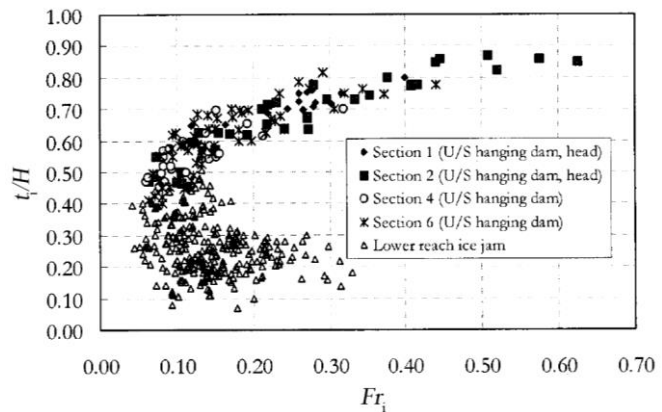
Figure 11. Relationship between
Fr_i and t_i/H of Hequ reach

5   CONCLUSIONS

With real ice experiments, the ice jam accumulation process before the inlet of the inverted siphon was studied. With an ice discharge of 0.12 L/s, it is shown that the larger the Froude number under the ice jam (Fr_i), the larger the dimensionless ice jam thickness (t_i/H) will be. The ice jam thickness (t_i) is not always increased. When the Froude number of the upstream open channel is large enough (about 0.1 in the experiments), the ice jam thickness (t_i) has a tendency to decrease, as shown in Figure 7. The ice supply is also an important factor for the ice jam thickness, an insufficient ice supply may lead to opposite results, just as in the lower Hequ reach of Yellow River.

The relationship between the dimensionless t_i/H and Fr_i is also investigated in this paper. And a linear equation with the two coefficients k and b is found to describe the ice jam thickness distribution along the channel. And the value of the coefficient k is in the range between 1.832 and 2.258 (mean value is 1.940), the value of the coefficient b is in the range between -0.044 and -0.094(mean value is -0.054).

These analysis results may help the ice jam prevention and the safe operation of similar water diversion projects in a high latitude area during ice period.

ACKNOWLEDGEMENTS

REFERENCES

Ashton, G. D (2011). River and lake ice thickening, thinning, and snow ice formation [J]. Cold Regions Science and Technology, 68(1): 3-19.

Ashton, G. D. (2008). Ice entrainment through submerged gate [C]. 19th IAHR International Symposium on Ice. Vancouver, British Columbia, Canada, 129-138.

Beltao, S., Carter, T. and Rowsell, R. (2012) Measurements and analysis of ice breakup and jamming characteristics in the Mackenzie Delta, Canada [J].Cold Regions Science and Technology, 82(4): 570-576.

Beltaos S. (2008). Progress in the study and management of river ice jams [J]. Cold Regions Science and Technology, 51(1): 2-19.

Dow, K. E., Hicks, F. E. and Steffler, P. M. (2011). Experimental investigation of the pressure distribution beneath a floating ice block [J]. Journal of Hydraulic Engineering, ASCE, 137(4): 399-411.

Fu, H., Yang, K. L. and Wang, T. (2010). Progress in the study of river ice hydraulics [J]. South-to-North Water Transfers and Water Science and Technology, 8(1): 14-18.

Fu, H., Yang, K. L. and Guo, Y. X. (2013a). An experimental study on ice jam prevention of typical inverted siphon for South- to-North Water Diversion Project [J]. Advances in Water Science, 24(5): 736-740.

Fu, H., Yang, K. L. and Tan, S. W. (2013b). Development and application of low temperature ice-hydrodynamics experiment platform [J]. Journal of Hydraulic Engineering, 44(3): 355-360.

Fu, H., Guo, X.L., and Yang, K.L. (2017). Ice accumulation and thickness distribution before inverted siphon[J]. Journal of Hydrodynamics, Ser.B, 29(1): 61-67.

Guo, X. L., Yang, K. L. and Fu, H. (2013). Simulation and analysis of ice processes in an artificial open channel [J]. Journal of Hydrodynamics, 25(4): 542-549.

Matsumoto, K., Koshizuka, M. and Honda, M. (2014). Measurement on nano scale by scanning probe microscope for obtaining real ice adhesion force [J]. International Journal of Refrigeration, 41(5): 181-189.

Michel, B. (1984). Comparison of field data with theories on ice cover progression in large rivers [J]. Canadian Journal of Civil Engineering, 11(4): 798-814.

Shen, H. T. (2010). Mathematical modeling of river ice processes [J]. Cold Regions Science and Technology, 62(1): 3-13.

Sui, J., Wang, J. and He, Y. (2010). Velocity profiles and incipient motion of frazil particles under ice cover [J]. International Journal of Sediment Research, 25(1): 39-51.

Sui, J., Karney, B. and Fang, D. (2005). Variation in water level under ice-jammed condition–Field investigation and experimental study [J]. Nordic Hydrology, 36(1): 65-84.

Sui, J., Karney, B. and Sun, Z. (2002). Field investigation of frazil jam evolution–A case study [J]. Journal of Hydraulic Engineering, ASCE, 128(8): 781-787.

Wang, J., Shi, F. Y. and Chen, P. P. (2015). Impact of bridge pier on the stability of ice jam [J]. Journal of Hydrodynamics, 27(6): 865-871.

Wang, J., Chen, P. P. and SUI, J. Y. (2011). Progress in studies on ice accumulation in river bends [J]. Journal of Hydrodyna- mics, 23(6): 737-744.

Yamazaki, M., Koyama, S. and Ken-Ichi, H. (2014). Accumulation of frazil slush and velocity distribution under the ice cover [J]. Journal of Dynamic Systems Measurement and Control, 136(3): 696-706.

Zhang, Y., Li, G. M. (2014). Influence of south-to-north water diversion on major cones of depression in North China Plain. Environ Earth Science, 71: 3845–3853.